2011 American Control Conference
on O'Farrell Street, San Francisco, CA, USA
June 29 - July 01, 2011

A Distributed Predictive Control Approach to Building Temperature Regulation

Yudong Ma*, Garrett Anderson*, Francesco Borrelli*

Abstract— **We study the problem of temperature regulation in a network of building thermal zones. The control objective is to keep zone temperatures within a comfort range while consuming the least energy by using predictive knowledge of weather and occupancy. First, we present a simplified two-mass nonlinear system for modeling thermal zone dynamics. Model identification and validation based on historical measured data are presented. Second, a distributed model-based predictive control (DMPC) is designed for optimal heating and cooling. The DMPC is implemented by using sequential quadratic program and dual decomposition. Simulation results show good performance and computational tractability of the resulting scheme.**

I. INTRODUCTION

The building sector consumes about 40% of the energy used in the United States and is responsible for nearly 40% of greenhouse gas emissions [12]. It is therefore economically, socially, and environmentally significant to reduce the energy consumption of buildings.

This work focuses on the modeling and predictive control of networks of thermal zones. The system considered in this manuscript consists of an air handling unit (AHU) and a set of variable air volume (VAV) boxes which serves a network of thermal zones. The AHU is equipped with a cooling coil, a damper, and a fan. The damper mixes return air and outside air. The cooling coil cools down the mixed air, and the fan drives the air to the VAV boxes. Each VAV box has a damper controlling the mass flow rate of air supplied to thermal zones. A heating coil in each VAV box can reheat the supply air when necessary.

The paper is divided in two parts. The objective of the first part is to develop low-order models suitable for real-time predictive optimization. In this work we model the system as a network of two-masses nonlinear systems. We present identification and validation results based on historical data collected from Bancroft Library at the University of California, Berkeley. The results are promising and show that the models well capture thermal zone dynamics when the external load (due to occupancy, weather, and equipment) is minor. Historical data are then used to compute the envelop of the external load by comparing nominal models and measured data when external disturbances are not negligible.

In the second part, a distributed model-based predictive control (DMPC) is designed for optimal heating and cooling.

* Y. Ma, F. Borrelli, and G. Anderson are with the Department of Mechanical Engineering, University of California, Berkeley, CA 94720-1740, USA. E-mail: {myd07, fborrelli, gandersen}@berkeley.edu.

The size of the centralized predictive control problem rapidly grows when a realistic number of rooms is considered. Therefore the real time implementation of an MPC scheme is a challenge for the low-cost embedded platforms which are used for HVAC control algorithms. The techniques presented in this paper enable the implementation of an MPC algorithm by distributing the computational load on a set of VAV box embedded controllers. Compared to existing DMPC schemes [3], the proposed method is tailored to the specific class of problem considered. In particular it makes use of sequential quadratic programming (SQP) [14], [4] and dual decomposition [9] to handle the system nonlinearities and the decentralization, respectively.

The main idea of dual decomposition is to take advantage of the separability of the dual lagrangian problem for certain classes of problems. By doing so, the dual problem is solved iteratively by updating dual and primal variables in a decentralized fashion. In this paper we show that if the centralized MPC problem is properly formulated, the resulting primal and dual update laws can be explicitly computed. Simulation results show good performance and computational tractability of the resulting scheme.

We remark that the evaluation of optimal controllers for building climate regulation has been studied in the past by several authors (see [15], [5] and references therein). Compared to existing literature, this paper focuses on distributing the computational load on multiple, low cost, embedded platforms.

The paper is organized as follow. Section II introduces the general system and the simplified thermal zone model. In Section III the distributed MPC control algorithm is outlined. A numerical example is presented in Section IV. Finally, conclusions are drawn in Section V.

II. SYSTEM MODEL

Objective of this section is to introduce a simplified HVAC system architecture and develop a control oriented model for it. We consider an air handling unit (AHU) and a fan serving multiple variable air volume (VAV) boxes controlling air temperature and flows in a network of thermal zones (next called "rooms" for brevity). Figure 1 depicts the system architecture: the AHU uses a mixture of outside air and return air to generate cool air by using a cooling coil (usually driven by chilled water, see [11] for optimal generation of chilled water). The cool air then is distributed by a fan to VAV boxes connected with each room. The damper position in the VAV box controls the mass flow rate of air entering a room. In

978-1-4577-0081-1/11/$26.00 ©2011 AACC

addition, a heating coil in the VAV box is used to warm up the supply air if needed.

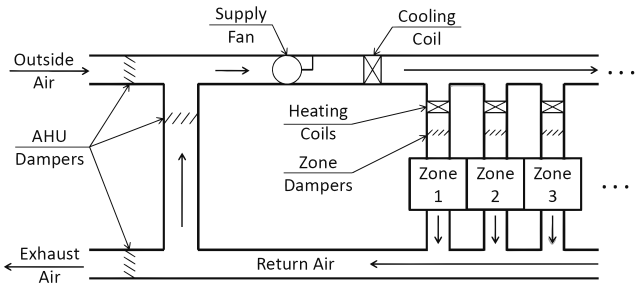

Fig. 1: System scheme

In order to develop a simplified yet descriptive model, the following assumptions are introduced.

- A1 The system pressure dynamics are not considered.
- A2 The dynamics of each component (AHU, VAV boxes and fan) are neglected. This implies that the supply air temperature and flow set points are tracked perfectly.
- A3 Air temperature is constant through the ducts.
- A4 The amount of air exiting the rooms is the same as the amount of air entering the rooms.

A. Simplified System Model

We use an undirected graph structure to represent the rooms and their dynamic couplings in the following way. We associate the i-th room with the i-th node of a graph, and if an edge (i, j) connecting the i-th and j-th node is present, the room i and j are subject to direct heat transfer. The graph $\mathcal{G}$ will be defined as

$$\mathcal{G} = (\mathcal{V}, \mathcal{A}), \tag{1}$$

where $\mathcal{V}$ is the set of nodes (or vertices) $\mathcal{V} = \{1, \ldots, N_v\}$ and $\mathcal{A} \subseteq \mathcal{V} \times \mathcal{V}$ the set of edges (i, j) with $i \in \mathcal{V},\ j \in \mathcal{V}$. We denote $\mathcal{N}^i$ the set of neighboring nodes of i, i.e., $j \in \mathcal{N}^i$ if and only if $(i, j) \in \mathcal{A}$.

Now consider a single room $j \in \mathcal{V}$. The air enters the room j with a mass flow rate $\dot{m}_s^j$ and temperature T_s^j. The temperature of air supplied to room j (T_s^j) is controlled by the cooling ΔT_c generated at the AHU, the heating ΔT_h^j at the reheating coils in the VAV box, and the damper position δ in the AHU sytem:

$$T_s^j = \delta T_r + (1 - \delta) T_{oa} - \Delta T_c + \Delta T_h^j, \tag{2}$$

where T_{oa} is the outside air temperature and T_r is the return air temperature calculated as weighted average temperature of return air from each room ($\sum_{i\in\mathcal{V}} \dot{m}_r^i T_r^i / \sum_{i\in\mathcal{V}} \dot{m}_r^i$). In (2) δ is the AHU damper position. The return air is not recirculated when $\delta = 0$, and no outside fresh air is used when $\delta = 1$. δ can be used to save energy through recirculation but it has to be strictly less than one to guarantee a minimal outdoor fresh air delivered to the rooms.

We model the room as a two-mass system. C_1^j is the fast-dynamic mass (e.g. air around VAV diffusers) that has lower thermal capacitance, and C_2^j represents the slow-dynamic mass (e.g. the solid part which includes floor, walls and furniture) that has thermal capacitance. We remark that the phenomenon of fast and slow dynamics has been observed in [6]. The thermal dynamic model of a room is:

$$C_1^j \dot{T}_1^j = \dot{m}_s^j c_p (T_s^j - T_1^j) + (T_2^j - T_1^j)/R^j + \sum_{i\in\mathcal{N}^j} (T_1^i - T_1^j)/R_{ij} + (T_{oa} - T_1^j)/R_{oa}^j + P_d^j, \tag{3a}$$

$$C_2^j \dot{T}_2^j = (T_1^j - T_2^j)/R_{12}^j, \tag{3b}$$

$$T_s^j = \delta \Big(\sum_{i\in\mathcal{V}} \dot{m}_s^i T^i\Big) / \Big(\sum_{i\in\mathcal{V}} \dot{m}_s^i\Big) + (1 - \delta) T_{oa} - \Delta T_c + \Delta T_h^j, \tag{3c}$$

$$T^j = T_1^j, \tag{3d}$$

where T_1^j and T_2^j are system states representing the temperature of the lumped masses C_1^j and C_2^j, respectively. T^j is the perceived temperature of room j, which is assumed to be equal to the temperature of the fast-dynamic mass C_1^j. $\mathcal{N}^j$ is the set of neighboring rooms of room j, R_{oa}^j is the thermal resistance between room j and outside air, and $c_p = 1012$ (J/kg $\cdot$ K) is the specific heat capacity of room air. R^j models the heat resistance between C_1^j and C_2^j, $R_{ij} = R_{ji}$ models thermal resistances between room i and the adjacent room j, and P_d^j is an unmeasured load induced by external factors such as occupancy, equipment, and solar radiation.

Figure 2 depicts the RC network corresponding to the graph $\mathcal{G}^0 = (\mathcal{V}^0, \mathcal{A}^0)$, where $\mathcal{V} = \{1, 2, 3, 4, 5\}$, $\mathcal{A} = \{(1,2), (1,3), (2,3), (3,4), (2,5), (4,5)\}$, and the neighboring nodes of the first node are $\mathcal{N}^1 = \{2, 3\}$.

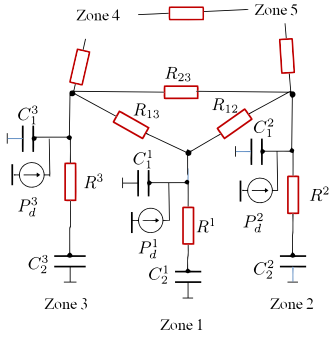

Fig. 2: Network of two-mass room model

The proposed approach is used to model the temperature dynamics of thermal zones in the Bancroft library located on the campus of University of California at Berkeley, USA. By using historical data we have identified the model parameters for each thermal zones and validated the resulting model.

Next we show the identification procedure and results by focusing on one thermal zone, a conference room (say $j = 1$). The dimension of the conference room is $5 \times 4 \times 3$ m, and it has one door and no windows. As a result, the effect of solar radiation is negligible. The major source of load derives from occupants and electronic equipment. The conference room has one neighboring office room ($\mathcal{N}^1 = \{2\}$).

The model parameters ($p = [C_1^1,\ C_2^1,\ R^1,\ R_{12},\ R_{oa}^1]$) are identified by using a nonlinear regression algorithm using measured data collected on July 4th, 2010 over 24 hours.

TABLE I: Identification results for conference room model on July 4th, 2010

Parameter	Value	Parameter	Value
C_1^1	9.163×10^3 kJ/K	R_{12}	2.000 K/kW
C_2^1	1.694×10^5 kJ/K	R_{oa}^1	57 K/kW
R^1	1.700 K/kW		

This corresponds to a Sunday when the conference room has no occupants ($P_d^1 = 0$). Measurements of room temperature (T^1), supply air temperature (T_s^1), mass flow rate of the supply air ($\dot{m}_s^1$), the neighboring room temperature (T^2), and outside air temperature T_{oa} are used for the identification. The identified parameters values are reported in Table I.

The identification results plotted in Figure 3 show that the proposed model successfully captures the thermal dynamics of the conference room without occupants. In Figure 3 the solid line depicts the measured room temperature trend and the dashed line is the room temperature predicted by model (3) when driven by the measured inputs.

The proposed model (3) with the identified parameters in Table I is validated against measurements during other weekends. Figure 4 plots the validation results for July 11th, 2010. One can observe that the predictions match well the experimental data.

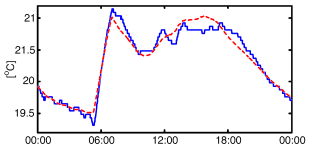

Fig. 3: Identification results of the thermal zone model (3)

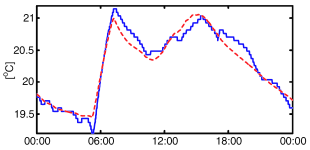

Fig. 4: Simplified room model validation

The load prediction $P_d(t)$ is important for designing predictive feedback controllers and assessing potential energy savings. We are currently investigating robust techniques, where $P_d(t)$ is modeled as a bounded time-varying uncertainty. Other approaches are available in the literature. For example, the authors of [10] proposed an agent-based model to simulate the occupants' behavior in a building.

The disturbance load envelopes can be learned from historical data, shared calendars, and weather predictions. For instance the conference room discussed earlier has two regularly scheduled group meetings around 10:00 and 14:00 every Wednesday. By using historical data we can observe this from the data. Figure 5 depicts the envelop-bounded load during all Wednesdays in July, 2010 (Figure 5). The envelop is computed as point-wise min and max difference between the measured data and the nominal model (i.e, model (3) with the identified parameters in Table I and $P_d^1 = 0$). Two

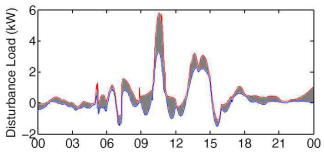

Fig. 5: Envelope bounds of disturbance load profile (Kw) for Wednesdays in July 2010

peaks can be observed in the disturbance load envelop in Figure 5, which corresponds to the two regularly scheduled group meetings. In the remainder of this paper we assume that a nominal prediction of disturbance load is available. Ongoing research is focused on stochastic MPC.

B. Constraints

The system (3) states and control inputs are subject to the following constraints (for all $j \in \mathcal{V}$):

1) $T_1^j \in [\underline{T},\ \overline{T}] = [20.6,\ 21.7]^o$C. Comfort range.
2) $m_s^j \in [\underline{\dot{m}},\ \overline{\dot{m}}] = [0.005,\ 5]$kg/s. The maximum mass flow rate of air supplied to a room is limited by the size of VAV boxes. The minimum mass flow rate is imposed to guarantee a minimal ventilation level.
3) $\Delta T_c^j \in [\underline{\Delta T_c},\ \overline{\Delta T_c}] = [0,\ 30]^o$C. The temperature decrement of the supply air (cooled by the cooling coil) is constrained by the capacity of the AHU.
4) $\Delta T_h^j \in [\underline{\Delta T_h},\ \overline{\Delta T_h}] = [0,\ 8]^o$C. The temperature increment of the supply air (heated by the heating coil) is constrained by the capacity of the VAV boxes.
5) $\delta \in [0,\ \overline{\delta}] = [0,\ 0.8]$. The AHU damper position is positive and less than $\overline{\delta}$ to make sure that there is always fresh outside air supplied to office rooms.

C. Model Summary

System equations (2)–(3) are discretized by using the Euler method with a sampling time Δt to obtain:

$$x^j(k+1) = f(x^j(k), u^j(k), u^c(k), d^j(k)) + \sum_{i \in \mathcal{N}^j} E_i^j x^i(k), \tag{4a}$$

$$y^j(k) = g(x^j(k)) = Cx^j(k), \tag{4b}$$

$$x^j(k) \in \mathcal{X},\quad u^j(k) \in \mathcal{U}^j,\quad u^c(k) \in \mathcal{U}^c, \tag{4c}$$

where $x^j = [T_1^j,\ T_2^j]$ is the state of the j-th room, $u^j = [\dot{m}_s^j,\ \Delta T_h^j]$ are the control inputs to the j-th VAV box, $u^c = [\Delta T_c,\ \delta]$ are the control inputs of the AHU system, and $d^j = [P_d^j,\ T_{oa}]$ is the disturbance assumed to be perfectly measured. The constraints (4c) are defined in Section II-B. Note that the room dynamics in the network are coupled through states (the second term in (4a)) and inputs (u^c is common to all rooms).

In the next section we will also use the following linearized version of model (4) around the trajectory $(\hat{x}_k^j,\ \hat{u}_k^j, \hat{u}_k^c,\ \hat{d}_k^j)\ \ \forall j \in \mathcal{V}$:

$$x^j(k+1) = A_k^j x^j(k) + B_k^j u^j(k) + B_k^c u^c(k) + D_k^j d^j(k) + \sum_{i \in \mathcal{N}^j} E_i^j x^i(k) + e_k^j, \tag{5a}$$

$$y^j(k) = Cx^j(k), \tag{5b}$$

$$x^j \in \mathcal{X},\quad u^j \in \mathcal{U}^j,\quad u^c \in \mathcal{U}^c, \tag{5c}$$

$$A_k^j = \left.\frac{\partial f}{\partial x_k^j}\right|_{\hat{x}_k^j},\ B_k^j = \left.\frac{\partial f}{\partial u_k^j}\right|_{\hat{u}_k^j},\ B_k^c = \left.\frac{\partial f}{\partial u_k^c}\right|_{\hat{u}_k^c},\ D_k^j = \left.\frac{\partial f}{\partial d_k^j}\right|_{\hat{d}_k^j}, \tag{5d}$$

$$e_k^j = -\hat{x}_{k+1}^j + A_k^j \hat{x}_k^j + B_k^j \hat{u}_k^j + B_k^c \hat{u}_k^c + D_k^j \hat{d}_k^j + \sum_{i \in \mathcal{N}^j} E_i^j \hat{x}_k^i. \tag{5e}$$

III. DISTRIBUTED MODEL PREDICTIVE CONTROL

A. Controller Design

In this section we formalize the MPC control problem and provide details of the decentralized MPC (DMPC) design. We are interested in solving the following optimization problem at each time step t:

$$\min_{\mathbf{U},\overline{\varepsilon},\underline{\varepsilon},\mathbf{X}} J(\mathbf{U},\overline{\varepsilon},\underline{\varepsilon},\mathbf{X}) = \sum_{j\in\mathcal{V}} \left\{ \sum_{k=0}^{N-1} \left(\|u^c_{k|t}\|_{R_c} + \|u^j_{k|t}\|_{R_u} \right) + \sum_{k=1}^{N} \left(\|x^j_{k|t} - T^j_{\text{ref}}\|_\sigma + \|\underline{\varepsilon}^j_{k|t}\|_\rho + \|\overline{\varepsilon}^j_{k|t}\|_\rho \right) \right\} \quad (6a)$$

subj. to:

$$x^j_{k+1|t} = f(x^j_{k|t}, u^j_{k|t}, u^c_{k|t}, d^j_{k|t}) + \sum_{i\in\mathcal{N}^j} E^j_i x^i_{k|t}, \quad \forall j\in\mathcal{V},\ k=0,1,\dots,N-1, \quad (6b)$$

$$y^j_{k|t} = Cx^j_{k|t},\ \forall j\in\mathcal{V},\ k=1,\dots,N, \quad (6c)$$

$$y^j_{k|t} \le \overline{T} + \overline{\varepsilon}^j_{k|t},\ \forall j\in\mathcal{V},\ k=1,\dots,N, \quad (6d)$$

$$y^j_{k|t} \ge \underline{T} - \underline{\varepsilon}^j_{k|t},\ \forall j\in\mathcal{V},\ k=1,\dots,N, \quad (6e)$$

$$u^j_{k|t}\in\mathcal{U}^j,\ u^c_{k|t}\in\mathcal{U}^c,\ \forall j\in\mathcal{V},\ k=0,\dots,N-1, \quad (6f)$$

$$\underline{\varepsilon}^j_{k|t}\ge 0,\ \overline{\varepsilon}^j_{k|t}\ge 0,\ \forall j\in\mathcal{V},\ k=1,\dots,N, \quad (6g)$$

where $\mathbf{U} = \{u^1_{0|t},\dots,u^1_{N-1|t},\dots,u^{N_v}_{0|t},\dots,u^{N_v}_{N-1|t}, u^c_{0|t},\dots,u^c_{N-1|t}\}$ is the set of control inputs at time t, $\mathbf{X} = \{x^1_{0|t},\dots,x^1_{N-1|t},\dots x^{N_v}_{0|t},\dots,x^{N_v}_{N-1|t}\}$ is the set of system states at time t, and $\|x\|_A = x^TAx$.

The cost function in (6) minimizes a weighted sum of the temperature deviation from the desired reference temperature T^j_{ref}, comfort constraint violations, and control efforts for each VAV box as well as AHU systems.

The constraint sets $\mathcal{U}^j$ and $\mathcal{U}^c$ are defined according to Section II-B. In (6) $x_{k|t}$ denotes the state vector at time $t+k\Delta t$ predicted at time t obtained by starting from the current state $x_{0|t}=x(t)$ and applying the input sequence $\mathbf{U}$ to the system model (6b).

Let the optimal solution of problem (6) at time t be $\mathbf{U}^\star = \{u^{\star 1}_{0|t},\dots,u^{\star 1}_{N-1|t},\dots,u^{\star N_v}_{0|t},\dots,u^{\star N_v}_{N-1|t}, u^{\star c}_{0|t},\dots,u^{\star c}_{N-1|t}\}$. Then, the first step of $\mathbf{U}^\star$ is implemented to system (4) $u^j(t)=u^{\star j}_{0|t},\ u^c(t)=u^{\star c}_{0|t}$.

The optimization (6) is repeated at time $t+\Delta t$, with the updated new state $x_{0|t+\Delta t}=x(t+\Delta t)$, yielding a *moving or receding horizon control* strategy.

The optimization problem (6) has quadratic cost subject to nonlinear constraints. The size of the nonlinear optimization problem rapidly grows when a realistic number of rooms is considered. In order to reduce the time to solve the optimization problem (6), we apply sequential quadratic programming (SQP) and dual decomposition. Next we show the main idea for both techniques and implementation details for the specific class of problems considered in this paper.

SQP procedure is an efficient method to solve nonlinear programming problems [4], [14]. The basic idea is to linearize the nonlinear optimization problem around a candidate optimal trajectory in order to obtain a quadratic program (QP). The QP optimal solution is used to update the candidate optimal trajectory. Linearization and QP solution are iteratively executed until convergence is achieved [4].

The concept of dual decomposition traces back to 70's [9], and it has been extensively studied since then [2], [16]. For specific classes of optimization problems, the lagrangian dual functions are separable, and therefore the optimal solutions can be computed in a decentralized fashion. The dual decomposition procedure guarantees zero duality gap and global convergence when the optimization problem is convex [9].

The optimization problem (6) is solved as follow.

1) Problem (6) is linearized by replacing the nonlinear system dynamic (6b) with the linearized ones (5).
2) The dual problem of the linearized version of Problem (6) is formulated where the dual variables λ, $\overline{\mu}$ and $\underline{\mu}$ are assigned to the constraints (6b), (6d), (6e), respectively. The dual problem can be formulated as follow.

$$\max_{\lambda,\underline{\mu},\overline{\mu}} \min_{\mathbf{U},\underline{\varepsilon},\overline{\varepsilon},\mathbf{X}} J + L^l + L^u + L^f \quad (7a)$$

subj. to

$$u^j_{k|t}\in\mathcal{U}^j,\ \ u^c_{k|t}\in\mathcal{U}^c, \quad \forall j\in\mathcal{V},\ \ k=0,1,\dots,N-1, \quad (7b)$$

$$\underline{\varepsilon}^j{}_{k|t}\ge 0,\ \ \overline{\varepsilon}^j{}_{k|t}\ge 0,\ \ \overline{\mu}^j_k\ge 0,\ \ \underline{\mu}^j_k\ge 0, \quad \forall j\in\mathcal{V},\ \ k=1,2,\dots,N, \quad (7c)$$

where J is the cost defined in (6a), $L^u = \sum_{j\in\mathcal{V}}\sum_{k=1}^N \overline{\mu}^j_k(Cx^j_{k|t} - \overline{T} - \overline{\varepsilon}^j_{k|t})$ is the dual term corresponding to constraint (6d), $L^l = \sum_{j\in\mathcal{V}}\sum_{k=1}^N(\underline{\mu}^j_k(-Cx^j_{k|t}+\underline{T}-\underline{\varepsilon}^j_{k|t})$ is the term for constraint (6e), and $L^f = \sum_{j\in\mathcal{V}}\sum_{k=1}^N \lambda^{j\,T}_k(A^j_kx^j_{k|t} + B^j_ku^j_{k|t}+B^c_ku^c_{k|t}+D^j_kd^j_{k|t}+\sum_{i\in\mathcal{N}^j}E^j_ix^i_{k|t}+e^j_{k|t}-x^j_{k+1|t})$ is the term for constraint (6b).
3) We note that cost function and constraints in problem (7) are separable in the primal variables. This special structure allows us to solve problem (7) in a distributed way as described next.
4) For a fixed set of dual variables ($\lambda^{\mathbf{j}p}$, $\underline{\mu}^{\mathbf{j}p}$, $\overline{\mu}^{\mathbf{j}p}$), the minimization problem involving the primal variables in (7) is solved explicitly as:

$$x^j_{k|t}{}^{p+1} = (2\sigma T^j_{\text{ref}} - (\overline{\mu}^{j\,p}_k - \underline{\mu}^{j\,p}_k)C^T - A^{j\,T}_k\lambda^{j\,p}_k + \lambda^{j\,p}_{k-1} - \sum_{i\in\mathcal{N}^j} E^{i\,T}_j\lambda^{i\,p}_k)/2\sigma, \quad (8a)$$

$$\underline{\varepsilon}^j_{k|t}{}^{p+1} = \mathcal{P}\left[\underline{\mu}^{j\,p}_k/2\rho\right]_{R_+},\ \overline{\varepsilon}^j_{k|t}{}^{p+1} = \mathcal{P}\left[\overline{\mu}^{j\,p}_k/2\rho\right]_{R_+}, \quad (8b)$$

$$\forall j\in\mathcal{V},\ \ \forall k=1,2,\dots,N,$$

$$u^j_{k|t}{}^{p+1} = \mathcal{P}\left[-\lambda^{j\,pT}_k B^j_k/2R_u\right]_{\mathcal{U}^j}, \quad (8c)$$

$$u^c_{k|t}{}^{p+1} = \mathcal{P}\left[-\sum_{j\in\mathcal{V}}\lambda^{j\,pT}_k B^j_k/2R_c\right]_{\mathcal{U}^c}, \quad (8d)$$

$$\forall j\in\mathcal{V},\ \ \forall k=0,1,\dots,N-1,$$

where $\mathcal{P}[\star]_{\mathcal{S}}$ is the operation of projecting $\star$ onto the convex set defined by $\mathcal{S}$ [7], and R_+ is the set of nonnegative real numbers.

5) By using the primal variables in (8), the dual variables are updated by using the projection subgradient method [7], [13], [1]:

$$\lambda_k^{j\,p+1} = \lambda_k^{j\,p} + \alpha_\lambda g_{\lambda_k^j}, \tag{9a}$$
$$\forall j \in \mathcal{V}, \quad \forall k = 0, 1, \ldots, N-1,$$
$$\underline{\mu}_k^{j\,p+1} = \mathcal{P}\left[\underline{\mu}_k^{j\,p} + \alpha_{\underline{\mu}} g_{\underline{\mu}_k^j}\right]_{R_+}, \tag{9b}$$
$$\overline{\mu}_k^{j\,p+1} = \mathcal{P}\left[\overline{\mu}_k^{j\,p} + \alpha_{\overline{\mu}} g_{\overline{\mu}_k^j}\right]_{R_+}, \tag{9c}$$
$$\forall j \in \mathcal{V}, \quad \forall k = 1, 2, \ldots, N,$$

where g_λ, $g_{\overline{\mu}}$ and $g_{\underline{\mu}}$ are the subgradients of the dual variables in Problem (7) at ($\lambda^{\mathbf{j}p}$, $\underline{\mu}^{\mathbf{j}p}$, $\overline{\mu}^{\mathbf{j}p}$) [9]:

$$g_{\lambda_k^j} = A_k^j {x_{k|t}^j}^{p+1} + B_k^j {u_{k|t}^j}^{p+1} + B_k^c {u_{k|t}^c}^{p+1} + D_k^j d_{k|t}^j + \sum_{i \in \mathcal{N}^j} E_i^j {x_{k|t}^i}^{p+1} + e_{k|t}^j - {x_{k+1|t}^j}^{p+1}, \tag{10a}$$
$$\forall j \in \mathcal{V}, \quad \forall k = 0, 1, \ldots, N-1,$$
$$g_{\underline{\mu}_k^j} = -C{x_{k|t}^j}^{p+1} + \underline{T} - {\underline{\varepsilon}_{k|t}^j}^{p+1}, \tag{10b}$$
$$g_{\overline{\mu}_k^j} = C{x_{k|t}^j}^{p+1} - \overline{T} - {\overline{\varepsilon}_{k|t}^j}^{p+1}, \tag{10c}$$
$$\forall j \in \mathcal{V}, \quad \forall k = 1, 2, \ldots, N.$$

In (9) $\alpha_\star$ is the step length for the variable $\star$.

6) The QP (7) for Problem (6) at s^{th} SQP iteration is solved by iterating between primal variables computation (8) and dual variables computation (9)–(10). The solution of QP (7) then becomes the new candidate solution ($\mathbf{X^{s+1}}$, $\mathbf{U^{s+1}}$) for the original Problem (6). Since the QP (7) is feasible we have zero duality gap, and if the step lengths $\alpha_\star$ are constant and sufficiently small, the ϵ-bounded global optimal solution to the linearized version of Problem (6) can be obtained [7].
7) The model (4) is relinearized around the new candidate optimal trajectory ($\mathbf{X^{s+1}}$, $\mathbf{U^{s+1}}$), a new QP is formulated and the procedure is repeated until $\|\mathbf{U}^{s+1} - \mathbf{U}^s\|_2 \leq \kappa$, $\|\mathbf{X}^{s+1} - \mathbf{X}^s\|_2 \leq \kappa$.

In summary, the proposed optimization is solved by using two types of iterations: the outer iteration solves the original nonlinear optimization problem (6) by solving a sequence of QP's (7), and the inner iteration solves the QP's (7) in a distributed fashion by using dual decomposition.

It is well know that the selection of step length $\alpha_\star$ is critical to guarantee convergence of the algorithm. The authors in [4] point out that SQP with fixed stepsize only guarantees local convergence, and may fail if the starting point is far away from the optimal solution. Methods ensuring (global) convergence to local optima of SQP procedures are discussed in [4], [14].

IV. Simulation Results

This section presents the simulation results for a numerical example to show the effectiveness of the proposed controller design methodology. For a simpler interpretation of the results, the control variable δ is set to zero so that no return air from the room is recirculated.

We compare the proposed methodology with a baseline control logic (BC), which is a simplified version of a production control logic. The BC works as follows. The mass flow rate of the supply air ($\dot{m}_s$) is set to its minimum (0.005 kg/s) when all the room temperatures are within the comfort range. The temperature of the AHUn cooling air is increased linearly at a rate of 3.5 (^{o}C/hour) until it reaches the constraints defined in Section II-B. When a room temperature hits the lower bound, the supply air temperature will be adjusted by the heating coil in the corresponding VAV box so that the room temperature stays at the lower bound value. When a room temperature violates the upper constraints, the AHU supply air temperature is set to its minimum, and the mass flow rate of the supply air is controlled so that the room temperature is within the comfort range.

The numerical example considers a network of 15 rooms. All the rooms have the same model parameters as in Table I identified for the conference room in the Bancroft library in Section II. The undirected graph describing the topology of the room network is $\mathcal{G}_1 = (\mathcal{V}_1, \mathcal{A}_1)$, where $\mathcal{V}_1 = \{1, 2, \ldots, 15\}$, and $\mathcal{A}_1 = \{(1,2), (2,3), \ldots, (14,15)\}$.

The ambient weather information is downloaded from July 2nd 12pm to July 3rd 12pm, 2009 at UC Berkeley, and the temperature profile is plotted in Figure 6(a). Because of the warm weather, only cooling is critical in the considered scenario.

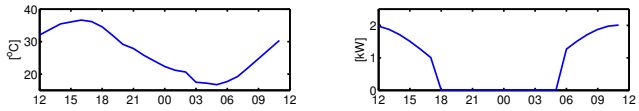

(a) Ambient temperature (T_{oa}) (b) Internal load profile

Fig. 6: Simulation setups

Figure 6(b) depicts the nominal internal load profile (P_{dn}) in our simulations. We assume that during 18:00 and 5:00 the next day, the rooms are empty without occupancy, leaving minimum internal load 0.01 kW due to lighting or other electrical devices. We use an internal load profile different for each room. In particular, we compute the internal load for room j as

$$P_d{}^j = (0.5 + 0.1j)P_{dn}, \quad j = 1, 2, \ldots, 15,$$

where P_{dn} is plotted in Figure 6(b).

In our simulations, the parameters for controllers in Section III are listed in Table II, and the constraints are defined in Section II-B. The sampling time Δt is chosen to be one hour, the predict horizon is one day $N = 24$, and the desired reference temperature (T_{ref}^j) is 21.6^{o}C. The step length ($\alpha_\star$) is selected heuristically in order to obtain convergence. Figure 7 shows the simulation results for the room network controlled by the baseline controller. The temperature of all rooms plotted in Figure 7(a) are within the comfort range defined by the dot lines. Before 22:10 all the room temperatures are on the upper bounds, and the baseline controller sets the supply

TABLE II: Parameters for the numerical example

param	value	param	value
R_c	0.9	R_u	diag(0.001, 7.5)
σ	0.001	ρ	1.6×10^4
N	24	α_λ	3.8×10^{-4}
$\alpha_{\underline{\mu}}$	3.8×10^{-4}	$\alpha_{\overline{\mu}}$	3.8×10^{-4}
κ	5×10^{-3}		

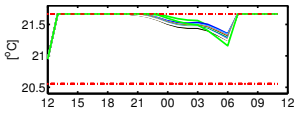

(a) Room temperature (T^j)

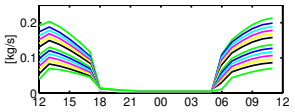

(b) Mass flow rate of the supply air from VAV box ($\dot{m}_s^j$)

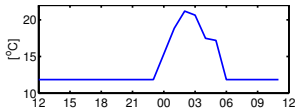

(c) Temperature of supply air from AHU (T_s^j)

Fig. 7: Baseline control

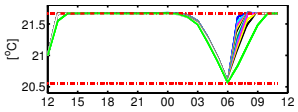

(a) Room temperature (T^j)

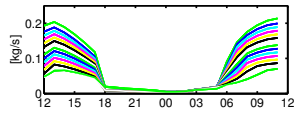

(b) Mass flow rate of the supply air from VAV box ($\dot{m}_s^j$)

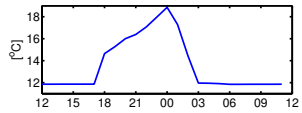

(c) Temperature of supply air from AHU (T_s)

Fig. 8: Distributed model predictive control

air temperature from AHU to its minimum (12^{o}C), and the supply air temperature increases linearly after 22:10 when all the rooms are comfortable.

The DMPC Algorithm in Section III is coded in Matlab® and runs on a PC with Intel Core Duo CPU 3.00GHz. The average runtime of the DMPC algorithm is 7 sec, and the maximum is 13 sec. The simulation results for the DMPC controller are presented in Figure 8.

The proposed DMPC controller cools down the room temperature to the lower bounds of the comfort range during the early morning (Figure 8(a)) while the baseline controller remains inactivated until the room temperature hits the upper bounds around 8:00 (Figure 7(a)). This *precooling* saves energy, since during the early morning the lower ambient temperature enables cooling coils to supply the required cooling air temperature at less cost (smaller ΔT_c in model (3c)). Moreover, the peak load shift at noon reduces the fan energy consumption (note that we use a quadratic penalty of supply air mass flow rate in (6a)).

DMPC controller applies a different supply air temperature resetting strategy (Figure 8(c)) compared to the baseline controller (Figure 7(c)). DMPC starts to increase the supply air temperature after 17:00 when the room temperatures are still on the upper bounds. After 17:00 the internal load is low and the fan works at low speed. In this regime it is more efficient to increase the fan power and use less chilled water in the cooling coils to maintain thermal comfort. With these unique features of DMPC, the total cost defined in (6a) is reduced by 10.2% compared to the baseline controllers.

V. CONCLUSIONS

In this study a simplified two-mass room model is presented. Validation results show that the model captures the thermal dynamics of a thermal zone with negligible external load. Based on this model and predictive information of loads due to occupancy and weather, a distributed model predictive control is designed to regulate thermal comfort. Recent research is focused on the study of the convergence of the SQP algorithm to local optima [8].

VI. ACKNOWLEDGMENTS

This material is supported by National Science Foundation under Grant No. 0844456. We thank Allan Daly, Miroslav Baric and Tommy Liu for constructive and fruitful discussions on system modeling and controller design.

REFERENCES

[1] Ya.I. Alber, A.N. Iusem, and M.V. Solodov. On the projected subgradient method for nonsmooth convex optimization in a hilbert space. *Mathematical Programming*, 81:23–35, 1998.

[2] D. P. Bertsekas and J. N. Tsitsiklis. *Parallel and Distributed Computation*, volume 290. Springer-Verlag, Englewood Cliffs, NJ, 1989.

[3] F. Borrelli, T. Keviczky, and G.E. Stewart. Decentralized constrained optimal control approach to distributed paper machine control. In *Decision and Control, 2005 and 2005 European Control Conference. CDC-ECC '05. 44th IEEE Conference on*, pages 3037 – 3042, Dec. 2005.

[4] S.P. Han. A globally convergent method for nonlinear programming. *Journal of Optimization Theory and Applications*, 22(3):297–309, July 1977.

[5] G.P. Henze, C. Felsmann, and G. Knabe. Evaluation of optimal control for active and passive building thermal storage. *International Journal of Thermal Sciences*, 43(2):173 – 183, 2004.

[6] J. Jang. *System Design and Dynamic Signature Identification for Intelligent Energy Management in Residential Buildings*. PhD thesis, University of California at Berkeley, 2008.

[7] B. Johansson, A. Speranzon, M. Johansson, and K.H. Johansson. Distributed model predictive consensus. Technical report, Automatic Control Lab, School of Electrical Engineering, Royal Institute of Technology (KTH). `http://citeseerx.ist.psu.edu/viewdoc/summary?doi=10.1.1.64.4190`.

[8] A. Kelman, Y. Ma, and F. Borrelli. Analysis of local optima in predictive control for energy efficient buildings. Technical report, University of California at Berkeley, 2011. `http://www.mpc.berkeley.edu/people/yudong-ma/files/KelmanCDC11.pdf`.

[9] L.S. Lasdon. Duality and decomposition in mathematical programming. *Systems Science and Cybernetics, IEEE Transactions on*, 4(2), Jul 1968.

[10] C. Liao and P. Barooah. An integrated approach to occupancy modeling and estimation in commercial buildings. In *American Control Conference (ACC), 2010*, pages 3130 –3135, Jun. 2010.

[11] Y. Ma, F. Borrelli, B. Hencey, B. Coffey, S. Bengea, and P. Haves. Model predictive control for the operation of building cooling systems. In *2010 American Control Conference*, pages 5106 –5111, Jun. 2010.

[12] J.M. McQuade. A system approach to high performance buildings. Technical report, United Technologies Corporation, Feb. 2009. `http://gop.science.house.gov/Media/hearings/energy09/april28/mcquade.pdf`.

[13] A. Nedic and A. Ozdaglar. Distributed subgradient methods for multi-agent optimization. *Automatic Control, IEEE Transactions on*, 54(1):48–61, Jan. 2009.

[14] J. Nocedal and S. J. Wright. *Numerical Optimization*, chapter 18. Springer-Verlag, 1999.

[15] F. Oldewurtel, A. Parisio, C.N. Jones, M. Morari, D. Gyalistras, M. Gwerder, V. Stauch, B. Lehmann, and K. Wirth. Energy efficient building climate control using stochastic model predictive control and weather predictions. In *2010 American Control Conference*, pages 5100–5105, Jun 2010.

[16] A. Rantzer. Dynamic dual decomposition for distributed control. In *American Control Conference, 2009*, pages 884 –888, Jun. 2009.